Journal of Sciences, Islamic Republic of Iran 20(2): **139-151 (2009)** http://jsciences.ut.ac.ir
University of Tehran, ISSN 1016-1104

Morphology and Petrogenesis of Pillow Lavas from the Ganj Ophiolitic Complex, Southeastern Kerman, Iran

A.R. Shaker Ardakani,[1,*] M. Arvin,[1] R. Oberhänsli,[2]
B. Mocek,[2,3] and S.H. Moeinzadeh[1]

[1]*Department of Geology, Faculty of Science, Shahid Bahonar University of Kerman, Kerman, Islamic Republic of Iran*
[2]*Department of Geology, Faculty of Science, University of Potsdam, Potsdam, Germany*
[3]*Department of Geology, Faculty of Science, University of Kansas, Lawrence, United States of America*

Received: 13 November 2008 / Revised: 25 February 2009 / Accepted: 9 March 2009

Abstract

The Upper Cretaceous Ganj complex, a part of the Jazmurian ophiolitic belt, is located on the western boundary of Jazmurian depression and separated from Kahnuj ophiolitic complex by north-south trending Jiroft fault. The complex consists of lava flows, pillow lavas, acidic plutonic and sedimentary rocks which are intruded by northwest-southeast trending dykes. It does not resemble a classical ophiolitic sequence due to lacking of intrusive crustal and mantle sections. The basaltic pillow lavas occur as flattened-tubular shape normal and mega sized bodies with bread crust crack surfaces. They show three textural zones from surface to interior: glassy, glassy and crystalline, and holycrystalline. Each zone characterized by different textures and varying assemblages of plagioclase ± olivine ± pyroxene and opaque. The glassy surface of the pillows frequently consists of one or rarely multiple rinds: sideromelane, dark tachylyte; and tachylyte with elongated vesicles. On Nb/Y versus Zr/TiO_2 and SiO_2 versus Nb/Y diagrams the pillow lavas plot in the field of basalt and sub-alkaline respectively. The relatively low immobile trace elements ratios are another sign of their tholeiitic nature. The absence of Eu anomaly on chondrite-normalized REE patterns suggests insignificances of plagioclase fractionation, or magma was relatively oxidized. They are similar to transitional basalts that lie between enriched MORB and OIB and some BABB. However enrichment in incompatible elements, depletion in Nb and low La/Nb ratios (0.94-1.81) are signature of BABB. They were formed by 15-30% partial melting of plagioclase lherzolite where fractionation was controlled by removal of olivine, spinel and clinopyroxene.

Keywords: Ganj ophiolitic complex; Pillow lava; MORB; Jazmurian ophiolitic belt

Introduction

Mesozoic ophiolites represent widespread fragments of the Neo-Tethyan Ocean that developed during the Triassic between Eurasia and Gondwanaland [5,69,70]. The Mesozoic suture zones in Iran are marked by significant aerial disruption of ophiolite related bodies. These suture zones are interpreted by numerous models.

* Corresponding author, Tel.: +98(341)3202233, Fax: +98(341)3222035, E-mail: shaker@mail.uk.ac.ir

Ricou [63] considered them as originating from a single ocean while others [5,32] believe that separate ophiolite alignments represent different ocean basins. This latter view is more consistent with abundant volcanic rocks, which represent different tectonic settings.

The Iranian ophiolites (Fig. 1) are part of the Middle Eastern Tethyan ophiolites and have a unique geographical position in joining the Asian ophiolites in the east (e.g. Pakistani and Tibetan) to the Mediterranean and Carpathian ophiolites in the west (e.g. Troodos, Greek and East European). On the basis of age and abundances, the Iranian ophiolites were classified into two main groups: the less abundant Paleozoic and more abundant Mesozoic ophiolites [2]. However, geographically they can be divided into four groups: (i) ophiolites of northern Iran along the Alborz range, (ii) ophiolites of Zagros Suture Zone, located near Neyriz and Kermanshah, which appear to be an extension of the Oman ophiolite abducted onto the Arabian continental crust, (iii) ophiolite complexes to the south of Jazmurian Depression which are known as Makran or Jazmurian ophiolitic belt. They are located to the north and south of Bajgan-Durkan microcontinent [41]. Those located to the north are represented by Band-e-Zeyarat / Dare-Anar, Ganj, Rameshk / Mokhtarabad complexes; whereas to the south a classic ophiolitic mélange of tectonic origin occurs. The ophiolites are mainly represented by small, disrupted fragments, but there are two intact or partly intact layered complexes, the Sorkhband and Rudan complexes dominated by ultramafic rocks. (iv) ophiolitic coloured mélange complexes of Central Iran (e.g. Baft, Shahr-Babak, Naein, Sabzevar and Tchehel-Kureh), which are marking the boundaries of the Central Iranian microcontinent (Fig. 1).

A tentative tectonic reconstruction considers that the Iranian Neo-Tethyan ophiolites were formed in three different structural zones: (1) a southern northwest-southeast trending belt which is called the Peri-Arabic belt [63] or southern Neo-Tethyan ocean [68,70], (2) the Central Iranian belt (trending N-S and E-W) which represents remnants of the Nain-Baft, Sabzevaran-Sistan oceans [43,81], and (3) the Jazmurian belt which trends northwest and east-west marking the remnants of the Makran ocean basin (Inner Makran suture of McCall and Kidd, [43]). The so-called Ganj ophiolitic complex (McCall and Kidd, [43]) belongs to this belt.

The aim of this paper is to present a descriptive view of pillow lavas morphologies and factors involved in their formation in the Ganj complex. Furthermore, their petrography, mineralogy and petrogenesis are also discussed.

Regional Geology

Among the most important revelations of the Paragon-Contech mapping of Makran (1976-1978) was the recognition of the Bajgan-Durkan complex (Bajgan-Durkan microcontinent) as continuation of the Sanandaj-Sirjan zone of Iran and the Bittlis massif of Turkey [37,41]. In this context the Sanandaj-Sirjan microcontinental sliver continues eastwards, right through Makran and is referred to as the Sanandaj-Sirjan-Bajgan-Durkan block (SS/BD) [42]. The SS/BD block consists of metamorphic rocks (garnitiferous schists, quartzites and marbles, e.g. Bajgan complex) of probable Early Paleozoic age or older, which are covered by highly deformed and disrupted Carboniferous to Lower Paleocene platform sequences dominated by shelf limestones (e.g., the Durkan complex).

The ophiolites to the north of the Bajgan-Durkan microcontinent (inner Makran spreading zone of McCall, [42]) are represented by the Band-e-Zeyarat /Dare-Anar (known also as Kahnuj ophiolite), Ganj, Rameshk / Mokhtarabad complexes [37,38,39,40]. They are mostly intact, only locally they form melanges, and with exception of the Ganj complex show classic sequences. They are all fault bounded and seem to belong to a large but dismembered complex [37].

Geological Setting

The Upper Cretaceous Ganj complex, a discontinuous north trending belt of 38 km length and 15 km width, is unusual in being dominated by intermediate and acidic dykes. Though, the Ganj complex has been

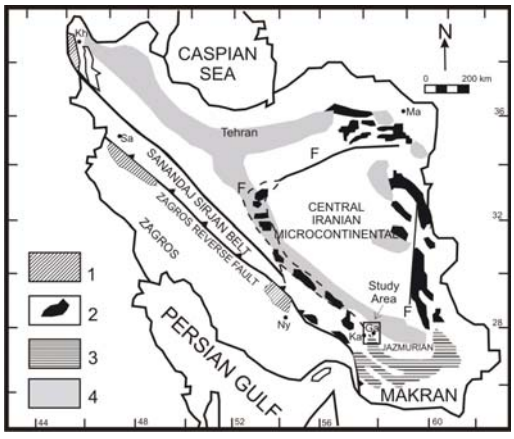

Figure 1. Map showing the distribution of the Iranian Mesozoic ophiolites: 1-Peri-Arabic belt, 2-Central Iranian belt, 3-Jazmurian belt, 4-Maastrichtian-Paleogene volcanic rocks. Ga = Ganj; Kh = Khoy; Ma = Mashhad; Ny = Neyriz; Sa = Sanandaj.

interpreted as an ophiolitic sequence [37], it does not resemble a classical ophiolitic sequence and lacks the intrusive crustal and mantle sections. The complex is bounded to the Kahnuj ophiolitic complex by the north-south trending Jiroft fault (Fig. 2).

The Ganj complex is predominantly of sheeted multiple dykes, locally curving, intruding country rocks which consist essentially of lava flows, but which has elements of plagiogranite (associated with minor gabbro) and turbiditic sediments. The volcanic rocks and dykes constitute approximately 85% of the outcrops. The former consist of pillowed lavas, brecciated and massive lava flows. They are mostly basic to acidic in composition and consist of basalt, basaltic andesite, keratophyre, quartz keratophyre, dacite, rhyodacite and rhyolite. Pillow lavas are mainly exposed to the south and less abundant in the northern part of the study area (Fig. 2). They are glandular and tubby in shapes, ranging from 0.2 to 7 meter in diameter. The pillow lavas do not show their actual geopethal structure, suggesting that they were tilted during their emplacement. The multiple northwest-southeast trending dykes are wide and forming sub-vertical zones up to 8 km long and 1.5 km wide. However, the early phases of dykes are thin and discontinuous. Locally, the ratio of dykes to rocks that they intruded may reach as high as 20:1. The dykes are mostly andesite and dacite feldspar porphyry with minor basaltic andesite, keratophyre and dacite-rhyodacite. The lavas and dykes of the Ganj ophiolitic complex contain low to medium grade hydrothermally altered material which was metamorphosed before tectonic emplacement and as in other ophiolitic complexes (ex, Pindos, Troodos) is considered to have occurred in the submarine environment. The alteration is a result of water/rock interaction at elevated temperatures through the convection process [76]. The lavas are generally altered to some extent to greenschist facies, whereas the dykes in parts are altered to zeolite facies assemblages**.** Plutonic rocks are acidic in composition and mostly consist of plagiogranite (tonalite, trondhjemite and albite granite). Minor gabbro is associated with plagiogranite, locally in an agmatite. K-Ar radiometric age dating indicates Senonian and Albian ages for plagioclase porphyry dykes and plagiogranites respectively [37]. Scarcely, Late Cretaceous sedimentary rocks as thinly bedded laminated sandstone, turbiditic siltstone, limestone and tuff occur as narrow screens between the dykes throughout the area.

Morphology of Pillow Lavas

Pillow lavas are important features of oceanic volcanism and their internal facies style helps to understand eruption processes, the evolution and emplacement conditions of the lava [4,30]. Pillow size is directly related to composition, viscosity and discharge rate of magma (with slope angle acting as a secondary controller), thermal endurance of the pillow or its ability to withstand fracturing during cooling [8, 47,64,75,82]. Steep slopes lead to premature detachment of pillow lavas, due to gravitational forces from the main feeder during emplacement [20,83], whereas gentler slopes provide a more even surface and longer time of stability for pillow expansion and growth [83].

Using the size classification scheme of Walker [83], the Ganj complex pillow lavas can be classified both as normal (<100 cm in length) and mega (>1 to 3 meters in length) pillows. They have different shapes and features, mostly flattened and tubular with bread crust crack surfaces (Fig. 3). The crack surfaces are directly related to their growth mechanism. Uniform and localized stretching of the outer crust generally creates small pillows with smooth-surface and unbroken chilled crusts [60,72,83]. Slower extrusion rates favor symmetrical spreading and toothpaste like pillow lavas with subsequent spreading and development of ruptures on chilled crust surfaces; as observed in the Ganj complex pillow lavas. The outer glassy surfaces of pillows are frequently consisting of one rind, rarely multiple rinds are observed. The rind is shiny black with thin cracks and ~ 1-2 cm thick. The multiple rinds in typical basaltic pillows consist of three layers, which from surface inwards are: (1) sideromelane, (2) dark tachylyte; and (3) tachylytic with elongated vesicles [28].

Several mechanisms have been proposed for the formation of multiple rind structures [28,49,74,87]. Initial interpretations focused on chilling of newly formed lava within tension cracks by seawater as mechanism for detachment of the outer rinds of pillows [18, 74]. Using this, Yamagishi [87] interpreted multiple rind structures as a result of repeated generation of shear joints between the outer solidifying crust and the molten interior. As a pillow forms by budding it develops a plastic skin, molten interior, evolved gases (as it is get cooled) and growth continues as long as a supply of hot lava is maintained. Studies also show that gas separation in subaerial pahoehoe in Hawaii could take place over an interval of 5-10 minutes or much less time in contact with water [79]. Internal pressure continues to build up within a pillow until it is suddenly decreased either by condensation of gases or drainage of lava through a new bud. This causes a pillow to implode or shrink and its plastic skin buckles inward or breaks at weakest points (e.g., at radial joints; Fig. 3e) and forms multiple-rind structures [26,28,45]. This view can be taken into

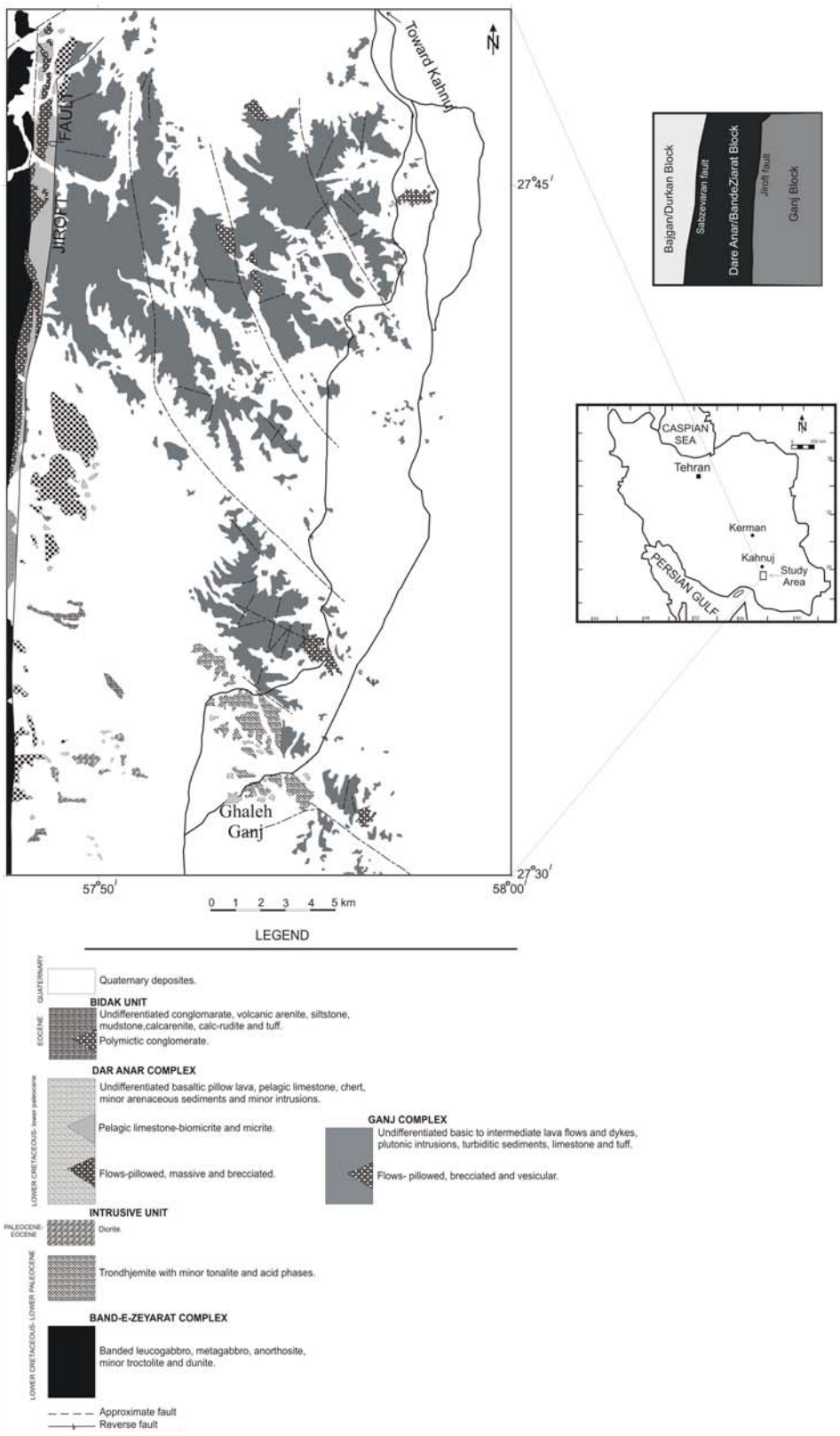

Figure 2. Geological map of the Ganj complex, southeast of Kahnuj, Kerman (modified from the Geological Map of Iran, 100,000 Series, sheet 7545).

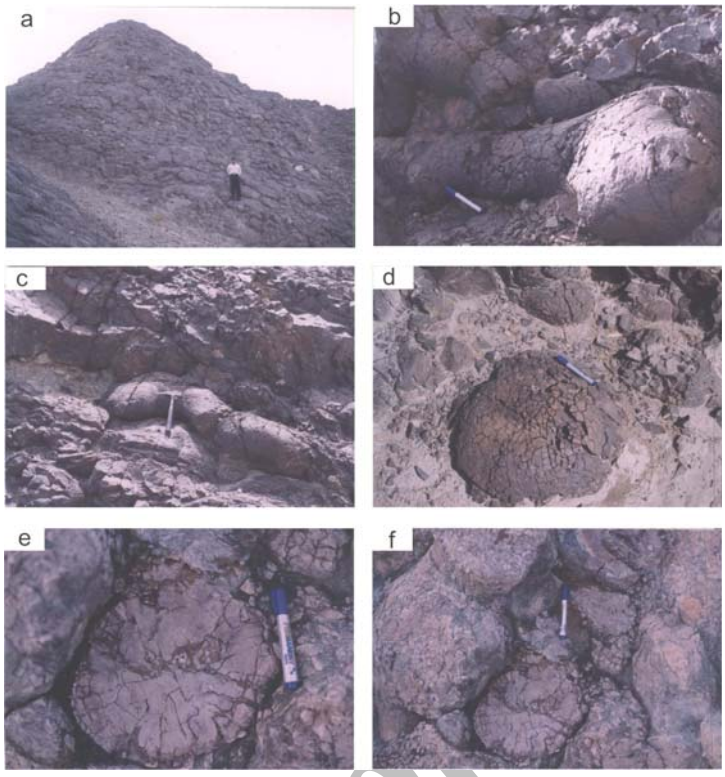

Figure 3. Field photographs showing different morphology of the pillow lava outcrops at Ganj complex pillow lavas. a) Flattened shape. (b, c) Tubular shape. (d) Bread crust crack surfaces. (e) Cross section of pillow showing internal radial and concentric cooling fractures. Note that edge of broken rind is roughly at right angle to external surface of pillow suggesting the break occurred at radial joints. (f) Spherical, oval and irregular shapes in cross section.

account for the formation of multiple rinds in the Ganj complex pillow lavas, where a series of radial fractures converge towards the centre, and probable shrinkage cracks developed during the cooling of the pillow lavas. Many of these fractures are now filled with secondary minerals such as calcite, prehnite-pumpellyite and chlorite. Furthermore, other factors may have been involved for the formation of multiple rinds such as: effusion rate, viscosity, temperature, total volume of extruded lava, and slope of underlying surface [28].

Throughout the Ganj complex the shapes of pillows vary considerably in cross section, from spherical, oval and elongated to irregular (Fig. 3f). These variations appear to have resulted from emplacement within spaces between preceding pillows and, in the case of irregular shaped bases, due to accommodation into the relief of earlier emplaced pillows [4]. Spaces between pillow lavas are filled with cements of hydrothermal origin by secondary minerals such as: calcite, chlorite and hyaloclastite breccias.

The morphology of the pillows observed in the Ganj complex is consistent with underwater observations made by Moore [48]. He proposed that the mechanism for pillow growth was not stretching of the outer skin but rather branching and lengthening through expansion, due to influx of fresh lava. Lava propagates forward as discrete lobes, which then instantaneously develop a visco-elastic skin as a result of surface cooling. Viscosity alone cannot dictate lava morphology, since its magnitude must change in order to cause variation in lava morphology [13, 14, 19-22].

Petrography

The Ganj complex pillow lavas can be divided in an aphyric (e.g., samples SE-11 and SE-13) and a phyric (e.g., samples SA-43-2, SE-10 and SE-12) group. Petrographic studies show obvious variations in crystal morphologies and textures between the chilled glassy outer rims and the holocrystalline cores. Three major textural zones were distinguished; similar textural zones were also reported from other parts of the world [3, 7, 31, 67]. All three zones show affect of alteration as assemblages of albite, chlorite, calcite, epidote, quartz,

prehnite, pumpellyite and uralite.

Zone (1) is vitrophyric at the rim composed of sheaf like radial clusters of plagioclase with scattered microphenocrysts of olivine and plagioclase in the interstices and opaque sitting in a glassy matrix. Plagioclase occurs as fine dendritic microlites, acicular (<0.25 mm), and rarely as subhedral skeletal laths up to 1.0 mm long. Commonly dendritic fibers or arms are observed at the plagioclase terminations. Olivine, as sparse skeletal microphenocrysts (0.5-1.0 mm), is observed in some samples. It is often altered and replaced by chlorite. Opaque minerals, in dendritic forms, are very abundant in zone1.

Zone (2) is a variolitic zone, characterized by skeletal crystals of plagioclase ± olivine ± clinopyroxene + opaque in a glassy matrix (hypohyaline texture). Plagioclase occurs as euhedral to subhedral elongated phenocrysts (up to 3 mm) and microlitic lath, with a variety of spherulitic forms, in the groundmass. Hollow plagioclase microlites are observed in this zone. Plagioclase often shows reaction rims/resorbed margins in the form of jagged ends and/or may have inclusions of the groundmass materials. Olivine occurs as microphenocrysts and micrloites in the groundmass. They are often altered and replaced by secondary minerals such as chlorite, calcite and prehnite-pumpellyite. Clinopyroxene occurs as subhedral to anhedral grains, < 0.1 mm, and is often replaced by uralite and chlorite. Opaque minerals appear as acicular and dendritic crystals in the groundmass.

Zone (3) is the inner holocrystalline basalt, which consists of plagioclase ± olivine ± clinopyroxene + opaque showing interstitial and to some extent flow textures. Plagioclase occurs as unzoned calcic euhedral to subhedral rectangular phenocrysts with rounded edges (up to 3 mm) and microlites with spherulitic forms in the groundmass and . Other characteristics of plagioclase are similar to zone 2. Olivine in zone 3 occurs as euhedral to subhedral phenocrysts (up to 3 mm) with various dendritic morphologies, and as microlite in the groundmass. Olivine phenocrysts are often altered and replaced by chlorite. Clinopyroxene occurs as anhedral to subhedral crystals with dendritic forms (up to 0.3 mm) which are replaced by uralite and chlorite in some cases. The clinopyroxenes together with plagioclase spherulites represent the variolitic texture in zone 3. Abundant dendritic opaque minerals occur between plagioclases.

Geochemistry

Nearly all the Ganj complex pillow lavas are altered to some extent to greenschist facies as a result of submarine hydrothermal alteration, a feature typical of other ophiolite basalts [56,58,73,82].

Studies of chemical changes due to alteration have revealed significant mobilities of most major oxides (except TiO_2 which may be considered relatively stable) and large ion lithophile (LIL) trace elements, such as Ba, Rb. These elements are unlikely to reflect primary composition [23,27]. On the other hand selected elements, particularly Zr, Nb, Ti, Y, Ta and rare earths (REE), may be used to characterize altered basic volcanics according to their petrological affinities and probable tectonic environment of formation [9,25,54, 71,84,86,88].

On the Nb/Y versus Zr/TiO_2 and SiO_2 versus Nb/Y diagrams [85] the Ganj complex pillow lavas plot mainly in the basalt and sub-alkaline fields respectively (Fig. 4). Further evidence of their sub-alkaline (tholeiitic) nature come from the low ratios of relatively immobile trace elements such as: Zr/Y (3.73-6.93), Th/Ta (1.18-1.73), La/Nb (0.94-1.81) and Nb/Y (0.08-0.57) [85] (Table 1). A wide range of Cr and Ni contents, relatively low TiO_2, P_2O_5 contents and low

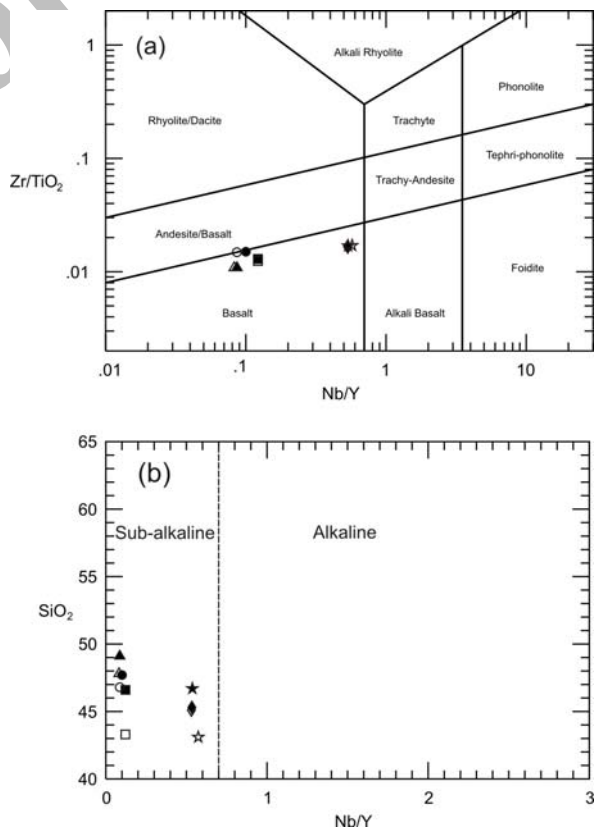

Figure 4. (a) Zr/TiO_2 versus Nb/Y and (b) SiO_2 versus Nb/Y diagrams for Ganj complex pillow lavas [85]. Symbols are the same as in Table 1.

Table 1. Representative analyses of the Ganj complex pillow lavas, Note: Major oxides in wt%; trace and rare elements in ppm; LOI= loss on ignition; FeO^*=total Fe as FeO

Sample	SA-43-2-C	SA-43-2-M	SE-10	SE-10-2	SE-11	SE-11-2	SE-12	SE-12-2	SE-13	SE-13-2
Position	Core	Margin	Core	Margin	Core	Margin	Core	Margin	Core	Margin
Texture	phyric	phyric	phyric	phyric	aphyric	aphyric	phyric	phyric	aphyric	aphyric
Symbol	△	▲	□	■	◇	◆	○	●		
SiO2	47.8	49.1	43.3	46.6	45.1	45.3	46.8	47.7	43.1	46.7
TiO2	1.265	1.233	1.271	1.229	1.826	1.594	1.146	1.068	1.702	1.579
Al2O3	14.3	14	15.7	15.3	16.2	14.9	17	17.6	16	15.7
FeO*	8.74	8.69	9.02	8.41	9.46	8.4	8.91	8.88	9.78	9.35
MnO	0.155	0.149	0.127	0.119	0.151	0.138	0.161	0.144	0.152	0.155
MgO	3.9	3.88	6.75	4.77	7.25	6.05	5.06	5.24	8.47	7.21
CaO	8.96	8.41	13.61	12.79	9.54	11.3	13.44	12.24	9.47	9.36
Na2O	5.53	5.33	3.16	4.59	2.92	3.76	3.48	3.54	2.91	3.84
K2O	0.13	0.17	0.36	0.16	1.78	1.37	0.1	0.15	1.5	0.79
P2O5	0.121	0.118	0.154	0.149	0.368	0.321	0.115	0.106	0.355	0.349
H2O	2.3	2.51	3.05	2.18	3.74	3.07	1.58	1.79	3.99	3.26
CO2	6.72	6.29	3.38	3.6	1.34	3.53	2.05	1.32	2.42	1.51
Total	99.921	99.88	99.882	99.897	99.675	99.733	99.842	99.778	99.849	99.803
LOI	9.02	8.8	6.43	5.78	5.08	6.6	3.63	3.11	6.41	4.77
FeO*/MgO	2.241026	2.2396907	1.3362963	1.7631027	1.30483	1.38843	1.76087	1.6946565	1.154664	1.29681
TiO2/P2O5	10.45455	10.449153	8.2532468	8.2483221	4.96196	4.96573	9.965217	10.075472	4.794366	4.5243553
Cr	33	35	346	332	277	272	254	309	454	361
Ga	17	14	19	15	16	15	16	17	15	17
Ni	11	10	167	140	143	137	126	201	249	176
V	234	250	198	205	188	178	193	178	172	177
Zn	87	86	63	47	68	61	49	54	101	79
Li	3.26	3.33	5.9	4.96	6.08	5.67			10	7.03
Rb	0.8	1.06	2.14	0.89	12.6	8.8	9	9	14.5	5.86
Sr	77	68.8	294	300	451	364	306	320	278	302
Y	22	20.1	22.4	21.7	26.9	23.2	22	19	25.1	24.2
Zr	82	80	98.1	95.5	182	158	102	96	174	160
Nb	1.82	1.74	2.72	2.65	14.3	12.4	1.9	1.9	14.4	13
Cs	0.01	0.02	0.01	0.01	0.02	0.02	0.01	0.02	0.04	0.02
Ba	5.91	6.83	34.3	26.9	77	69.2	44	19	91.5	64.9
La	3.3	2.88	4.31	4.29	13.5	11.6	3.003	3.016	13.9	13.5
Ce	9.17	8.47	12.4	12	30.2	26	10.1	9.93	30.5	28.4
Pr	1.52	1.4	1.96	1.89	3.97	3.38	1.636	1.61	3.88	3.77
Nd	8.05	7.61	9.96	9.64	17.3	15.1	8.11	7.99	16.9	16.1
Sm	2.71	2.6	3.01	3.01	4.5	3.84	2.449	2.398	4.29	3.98
Eu	1.12	1.05	1.15	1.09	1.59	1.37	1.006	0.999	1.44	1.44
Gd	3.72	3.38	3.85	3.78	5.11	4.41	3.052	3.036	4.79	4.62
Tb	0.66	0.58	0.66	0.63	0.83	0.72	0.5181	0.5147	0.79	0.75
Dy	4.13	3.93	4.26	4.23	5.35	4.62	3.449	3.403	4.96	4.65
Ho	0.91	0.82	0.91	0.89	1.09	0.96	0.718	0.7057	1.01	0.97
Er	2.64	2.36	2.64	2.54	3	2.72	2.06	2.024	2.9	2.65
Tm	0.37	0.34	0.37	0.35	0.42	0.37	0.35	0.36	0.4	0.39
Yb	2.33	2.25	2.38	2.32	2.76	2.38	1.914	1.879	2.58	2.46
Lu	0.37	0.33	0.35	0.34	0.41	0.36	0.268	0.2622	0.39	0.38
Hf	2.18	2.12	2.43	2.37	4.07	3.51	2.23	2.3	3.78	3.5
Ta	0.11	0.11	0.17	0.15	0.9	0.81	0.13	0.14	0.9	0.83
Pb	3.57	2.85	1.56	1	1.49	1.47			1.13	1.74
Th	0.19	0.18	0.2	0.2	1.13	0.97	0.18	0.19	1.1	1.03
U	0.17	0.21	0.13	0.17	0.43	0.39	0.18	0.2	0.4	0.34
Nb/Y	0.082727	0.0865672	0.1214286	0.1221198	0.5316	0.53448	0.086364	0.1	0.573705	0.5371901
Zr/Y	3.727273	3.9800995	4.3794643	4.4009217	6.7658	6.81034	4.636364	5.0526316	6.932271	6.6115702
Th/Ta	1.727273	1.6363636	1.1764706	1.3333333	1.25556	1.19753	1.384615	1.3571429	1.222222	1.2409639
La/Nb	1.813187	1.6551724	1.5845588	1.6188679	0.94406	0.93548	1.580526	1.5873684	0.965278	1.0384615
Eu/Eu*	1.08	1.08	0.99	1.03	1.01	1.02	1.12	1.13	0.97	1.03
(La/Yb)cn	1.01	0.92	1.32	1.3	3.51	3.5	1.12	1.15	3.86	3.94

TiO_2/P_2O_5 ratios (4.52-10.45) [78] equally point to a transitional tholeiitic nature. In trace element discrimination diagrams of the eruptive environments for basic rocks such as V versus Ti and Ce/Nb versus Th/Nb diagrams (Figs. 5 and 6) the Ganj complex pillow lavas show affinities to typical mid ocean ridge basalts (MORB) and back-arc basin basalts (BABB), rather than island-arc tholeiite (IAT) [1, 55, 66]. The Ce/Nb versus Th/Nb diagram (Fig. 6) is considered to be the best discriminant for tectonic environment and these ratios are interpreted to reflect source values [65].

The La/Nb ratio versus Y diagram provides useful discrimination between ocean ridge (with low, restricted La/Nb) and subduction-related eruptive settings [6, 17]. The La/Nb ratio provides an indication of LILE-enrichment in a subduction-related environment relative to HFSE [65]. The low La/Nb ratios of the Ganj complexe pillow lavas indicate that they are representative of a back-arc basin environment (rather than an arc) and are clearly distinguished from enriched MORB or intraplate oceanic flood lava flows with similar low Y contents [16] (Fig. 7). Comparison of geochemical patterns of the pillow lavas to MORB, island arcs and back arc basin basalts [53] may be made using the high ionic potential elements which are regarded immobile during alteration. Their normalized MORB multi-element diagrams (Fig. 8) show that the pillow lavas are enriched in large ion lithophile elements (LIL) relative to MORB. This enrichment is higher in aphyric relative to porphyritic pillows.

The chondrite-normalized rare earth element (REE) patterns (Fig. 9) show a relatively mild enrichment in light REEs (LREEs) relative to heavy REEs (HREEs). The low level enrichment in LREE decrease from aphyric [$(La/Yb)_{cn}$= 3.50-3.94)] to porphyric pillow lavas [$(La/Yb)_{cn}$= 0.92-1.32)]. The pattern lack the LREE typical depletion of N-type MORB and many island arc tholeiitic (IAT), but show similarities to T-type MORB and some back-arc basin basalts (BABB) [15, 29, 78]. The level of REE contents of aphyric and porphyric also correspond to those between E-MORB and OIB. The absence of a distinct Eu anomaly (Eu/Eu^* = 0.97-1.13), indicates that plagioclase fractionation was not significant, or that the magma was relatively oxidized.

For the petrogenetic discrimination of basalts, oceanic or not, Pearce and Peate [59] and Pearce [52] used two ratio plots of Th versus Nb (i.e. Th/Yb-Nb/Yb) as proxy to highlight the crustal contamination and Ti versus Nb (i.e. Ti/Yb-Nb/Yb) to highlight melting depth. The Th/Yb-Nb/Yb diagram (Fig. 10) indicates present day MORB with a slight evolution towards OIB, and interacted with continental crust during ascent or show a subduction component then they plot above the MORB-OIB array or on a vector at a steep angle to the array, reflecting selective Th addition [52]. On the Ti/Yb-Nb/Yb diagram (Fig. 11) N-MORB and E-MORB are obvious. The Ganj complex pillow lavas clearly show their MORB affinities with tendency towards both E-MORB and OIB compositions with no sign of crustal involvement, either direct crustal contamination or crustal recycling by subduction or via inherited subduction components in the lithosphere in Figures 10 and 11 [52].

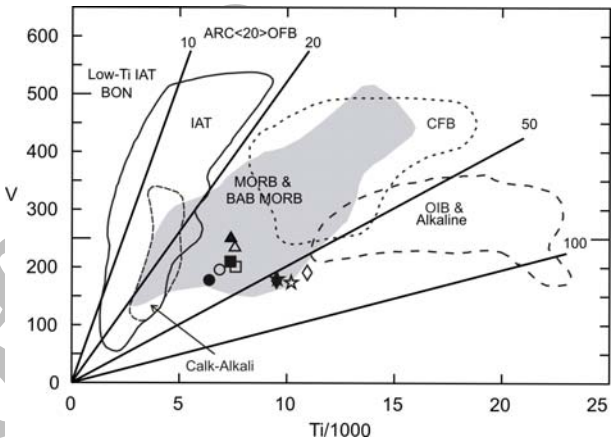

Figure 5. Ti versus V diagram of Shervais [71]. IAT = island arc tholeiitic, BAB = back-arc basin basalts, CFB = continental flood basalts, and OIB = oceanic island basalts. Symbols are the same as in Table 1.

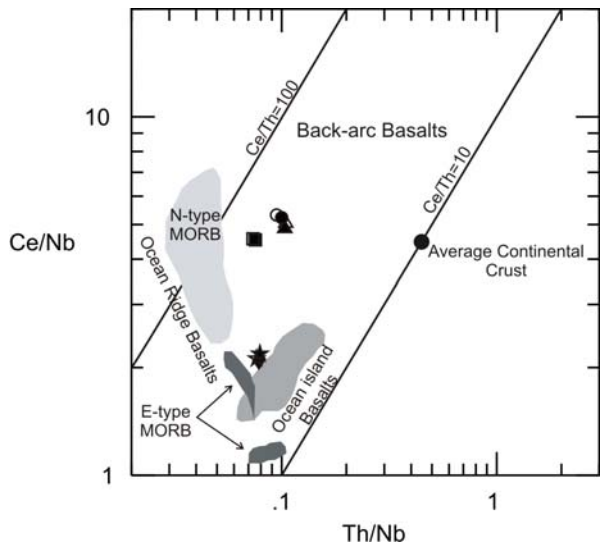

Figure 6. Ce/Nb versus Th/Nb diagram for the Ganj complex pillow lavas, fields are from Saunders and Tarney [66]. Symbols are the same as in Table 1.

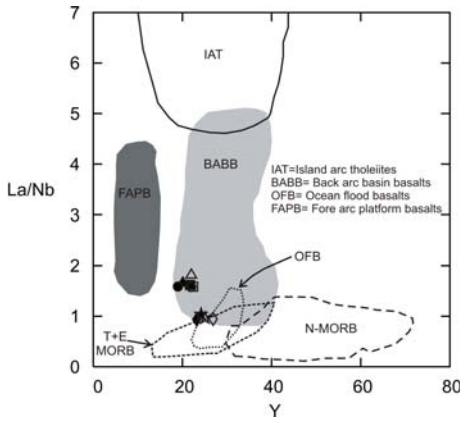

Figure 7. La/Nb versus Y plot [17] for the Ganj complex pillow lavas. Symbols are the same as in Table 1.

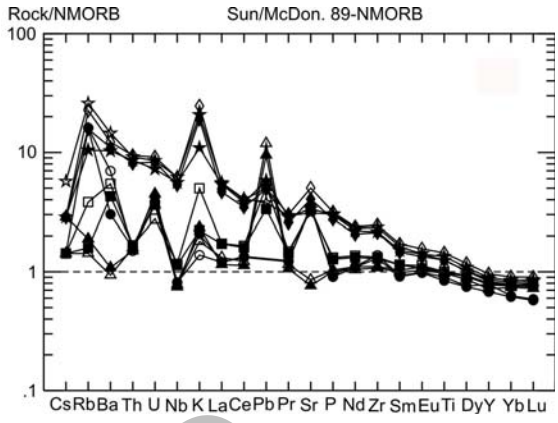

Figure 8. MORB-normalized multi-element plots for the Ganj complex pillow lavas, normalized values from Sun and McDonough, [77]. Symbols are the same as in Table 1.

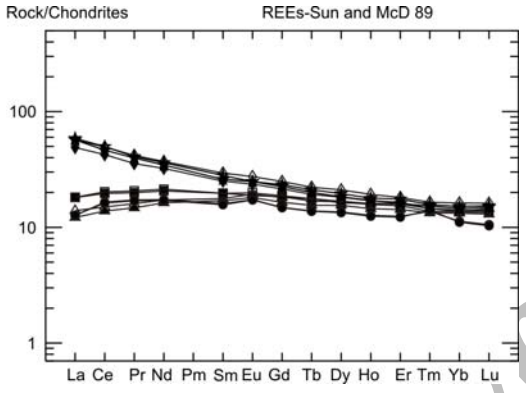

Figure 9. Chondrite-normalized REE patterns [77] for the Ganj complex pillow lavas. Symbols are the same as in Table1.

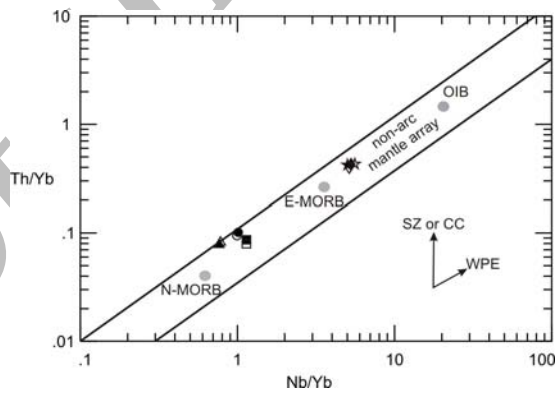

Figure 10. Th/Yb versus Nb/Yb diagram [59] of the Ganj complex pillow lavas., WPE= within-plate enrichment. SZ= subduction zone flux. CC= crustal contamination. N-MORB, E-MORB, and OIB from Sun and McDonough [77]. Symbols are the same as in Table 1.

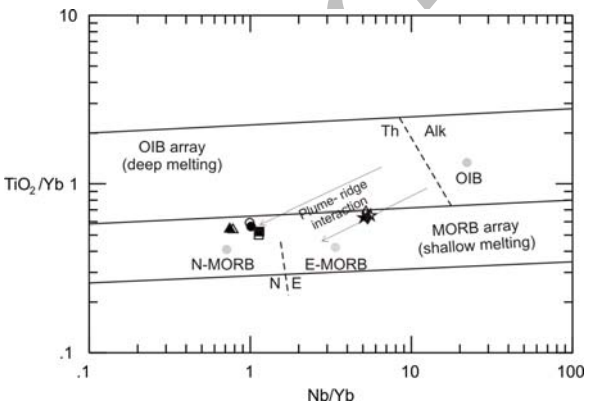

Figure 11. TiO_2/Yb versus Nb/Yb diagram (Pearce, 2008) of the Ganj complex pillow lavas, WPE: within-plate enrichment; SZ: subduction zone flux; CC: crustal contamination. N-MORB, E-MORB, and OIB fields from Sun and McDonough (1989). Symbols are the same as in Table 1.

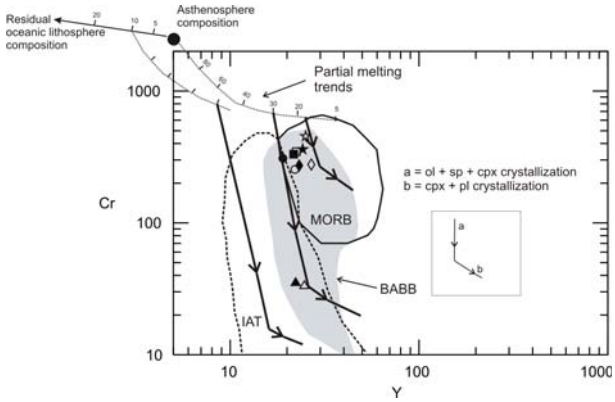

Figure 12. Cr-Y diagram [57] for the Ganj complex pillow lavas. Symbols are the same as in Table 1.

In a Cr versus Y diagram [55] the pillow lavas plot mainly in the MORB and BABB fields (Fig. 12). As it shows they formed as a result of 15-30% partial melting of plagioclase lherzolite and that they lie along the fractional crystallization trend that is controlled by removal of olivine, spinel, clinopyroxene. Similarly, Lippard et al. [33] suggested 20-30% partial melting to produce melt for the Cpx-phyric basalt unit of the Semail ophiolite [24].

Results and Discussion

Research on pillow lavas has focused on the processes of formation and propagation on the seafloor [45]. Studies on the morphology of pillow lavas have been carried out on freshly formed submarine pillows [87]. Ganj complex pillow basalts have been formed when hot, fluid basaltic lava rapidly cooled upon its contact with the cold seawater. This had effects not only on the textural and mineralogical features of the pillows, but due to different cooling rates of the lava, three broad textural zones were formed. These textural zones are from margins inward (1) a glassy crust; (2) incipient microcrystalline zone with feathery crystals, which gradually grade into zone (3) which is a holocrystalline inner part of pillow lava [45]. The presence of various mineral phases in these three zones reveals their development and crystallization sequence. Though these phases may vary in each sample, one can infer a general idea of mineral paragenesis in the Ganj complex pillow lava.

The abundance of olivine as phenocrysts and microlites even near glassy margin in the Ganj complex pillow lavas indicates a magnesium rich composition of the magma [50, 51]. The presence of olivine or plagioclase or both in the quenched outer glassy rim (zone 1) has been reported from recent oceanic basalts [46]. Crystal growth in zone 1 and in the outer part of zone 2 may have occurred under super cooled conditions in which the viscosity of the melt significantly reduced the diffusion rates [7]. For crystals to grow in euhedral shape, the melt temperature must be maintained at or just below the liquidus temperature for relatively long periods of time [7].

The assemblage of acicular plagioclase and clinopyroxene spherulites along with some individual dendritic laths of plagioclase in the pillow lavas, such as Ganj complex pillow lavas, has been interpreted as an indication of a cooling rate of 5-20°C/h for the middle and core zones of pillows [35, 44, 80]. The abundance of zoned crystals shows an almost inverse proportion to the ascent rate of magma and also the size of the magma chamber [15]. Thus, it seems the Ganj complex pillow lavas formed as magma rouse rapidly from its chamber with little or no time to form zoned crystals [15].

The formation of basaltic textures is depending from: cooling rate, fluid flow, liquid composition, nucleation and growth rates, heterogeneous nucleation, and settling or floating of crystals [45]. The occurrence of phenocrysts and microlitic plagioclase in the Ganj complex pillow lavas, show either different stages of a cooling history or, more likely, the effect of sudden changes in the degree of super-cooling [35] (ΔT), and the number of nuclei [34]. The nucleation rate or nucleation density is influenced by the cooling rate that in turn controls the differences in grain size. For example, low nucleation rate and high growth rate, will produce phenocrysts/megacrysts, whereas high nucleation and growth rate result microphenocrysts [45]. The wide range of plagioclase sizes in the Ganj complex pillow lavas; points to a high number of nuclei per unit volume present in the parent melt.

Geochemical data indicate that the Ganj complex pillow lavas are tholeiitic in composition and show similarities with transitional basalts between enriched MORB and OIB and some back arc basin basalts. However their enrichment in incompatible elements, depletion in Nb and low La/Nb ratios (0.94-1.81) are signature of BABB. They were probably formed by approximately 15-30% partial melting of mantel lherzolite. Aphyric basalts show more differentiated compositions and higher incompatible element contents than phyric lavas [10, 11, 12, 61, 62]. As observed in the Ganj complex, lavas with aphanitic textures are enrichment in LREE as compared to those with porphyritic textures. The absence of a distinct Eu anomaly in the Ganj complex pillow lavas suggests that plagioclase fractionation was not particularly significant, or it may indicate that the magma was relatively oxidized.

Acknowledgements

Financial support for chemical analyses was provided by Department of Geology at Potsdam University in Germany. A.R. Shaker Ardakani would like to express his special thanks and deep appreciation to Prof. F. Scherbaum (Head of Geology Department), Dr. U. Altenberger, Dr. C. Günter, C. Fischer at Potsdam University and Dr. F. Wombacher of Free University of Berlin for their helps in laboratory works. The authors are grateful to anonymous reviewers for critically reading the manuscript.

References

1. Arvin, M., Houseinipour, A., Babaei, A.A. and Babaie H.A. Geochemistry and tectonic significance of basalts in the Dare-Anar Complex: Evidence from the Kahnuj Ophiolitic Complex, Southeastern, Iran. *J. Sci. I. R. Iran.* **12**: 157-170 (2001).
2. Arvin, M. and Robinson P.T. The petrogenesis and tectonic setting of lava from the Baft ophiolitic mélange, southwest of Kerman, Iran. *Canad. J. Earth Sci.,* **31**: 824-834 (1994).
3. Banerjee, R. and Iyer S.D. Petrography and chemistry of basalts from the Carlsberg Ridge, *J Geol Soc India.,* **38**: 369-386 (1991).
4. Bear, A.N. and Cas R.A.F. The complex facies architecture and emplacement sequence of a Miocene submarine mega-pillow lava flow system, Muriwai, North Island, New Zealand. *J. Volcanol. Geotherm. Res.,* **160**: 1-22 (2007).
5. Berberian, M. and King G.C.P. Towards a palaeogeography and tectonic evolution of Iran. *Canad. J. Earth Sci.,* **18**: 210-65 (1981).
6. Bougault, H., Joron, J.L. and Treuil M. The primordial chondritic nature and large-scale heterogeneities in the mantle: Evidence from high and low partition coefficient elements in oceanic basalts. *Philos. Trans. R. Soc. London.,* **279**: 203-13 (1980).
7. Bryan, W.B. Morphology of quench crystals in submarine basalts, *J Geophys Res.,* **77**: 5812-5819 (1972).
8. Cas, R.A.F. Submarine volcanism: eruption style, products, and relevance to understanding the host rock successions to volcanic hosted massive sulphide deposits. *Econ. Geol.,* **87**: 511-541 (1992).
9. Daly, K.B. A study of the mafic plutons along the Bloody Bluff Fault in northeastern Massachusetts: Placing constraints on the tectonic environment using geochemical and petrologic analysis. M.Sc. thesis, Boston College, 157p (2003).
10. Dmitriev, L.V. Petrology of the basalts: Legs 45, 46, In: L. Dmitriev, J. Heirtzler et al. (Ed.), Initial Rep. *Deep Sea Drill. Proj.,* **46**: 143-150 (1978).
11. Dungan, M.A. and Rhodes J.M. Residual glasses and melt inclusions in basalts from DSDP Legs 45 and 46: Evidence for magma mixing, *Contrib. Miner. Petrol*., **67**: 417-431 (1978).
12. Dungan, M.A., Rhodes, J.M., Long, P.E., Blanchard, D.P., Brannon, J.C. and Rodgers K. The petrology and geochemistry of basalts from site 396, Legs 45 and 46 of the Deep Sea Drilling Project, In: L. Dmitriev, J. Heirtzler et al. (Eds.), Initial Rep. *Deep Sea Drill. Proj.,* **46**: 89-113 (1978).
13. Fink, J.H. and Griffiths R.W. Radial spreading of viscous-gravity currents with solidifying crust. *J. Fluid Mechan.,* **221**: 485-501 (1990).
14. Fink, J.H. and Griffiths R.W. A laboratory analog study of the morphology of lava flows extruded from point and line sources. *J. Volcanol. Geotherm. Res.,* **15**: 19-32 (1992).
15. Fisk, M.R. Depths and temperatures of mild ocean ridge magma chambers and composition of their source magmas, in ophiolites and oceanic lithosphere, edited by I G Gass, S J Lippard & A W Shelton, (Blackwell Sci Publ, Oxford). 17-23 (1984).
16. Floyd, P.A. Geochemical features of intraplate oceanic plateau basalts. In: Saunders, A. and Norry, M. (Eds.), Magmatism in ocean basins. *Geol. Soc. London Spec. Publ.,* **42**: 215-30 (1989).
17. Floyd, P.A., Kelling, G., Gocken, S.L. and Gocken N. Geochemistry and tectonic environment of basaltic rocks from the Miss ophiolitic uatern, south Turkey. *Chem. Geol.,* **89**: 263-80 (1991).
18. Fuller, R.E. Tensional surface features of certain basalt ellipsoids. J Geol **40**: 164-170 (1932).
19. Gregg, T.K.P. and Fink J.H. Quantification of submarine lava-flow morphology through analog experiments. *Geology,* **23**: 73-76 (1995).
20. Gregg, T.K.P. and Smith D.K. Volcanic investigations of the Puna Ridge, Hawaii, relations of lava flow morphologies and underlying slopes. *J. Volcanol. Geotherm. Res.,* **126**: 63-77 (2003).
21. Griffiths, R.W. and Fink J.H. Solidification and morphology of submarine lavas: a dependence on extrusion rate. *J. Geophys. Res.,* **97(19)**: 729-737 (1992a).
22. Griffiths, R.W. and Fink J.H. The morphology of lavas in planetary environments: predictions from analogue experiments. *J. Geophys. Res.,* **97**: 19739-19748 (1992b).
23. Hart, S.R., Erlank, A.J. and Kable E.J.D. Sea floor basalts alteration: some chemical and strontium isotopic effects. *Contrib. Mineral. Petrol.,* **44**: 219-30, (1974).
24. Hassanipak, A.A. and Ghazi A.M. Petrology, geochemistry and tectonic setting of the Khoy ophiolite, northwest Iran: implication for Tethyan tectonics. *J. Asian Earth Sci.,* **18**: 109-121 (2000).
25. Holm, P.E. The geochemical fingerprints of different tectonomagmatic environments using hygromagmatophile element abundances of tholeiitic basalts and basaltic andesites, *Chem. Geol.,* **51**: 303-323 (1985).
26. Hopgood, A.M. Radial distribution of soda in a pillow of spilitic lava from the Franciscan, California, *Am. J. Sci.,* **260**: 383-396 (1962).
27. Humphris, S.E. and Thompson G. Trace element mobility during hydrothermal alteration of oceanic basalts. *Geochim. Cosmochim. Acta.,* **42**: 127-136 (1978).
28. Kawachi, Y. and Pringle I.J. Multiple rind structure in pillow lava as an indicator of shallow water. *Bull. Volcanol.,* **50**: 161-168 (1988).
29. Keller, R.A., Fisk, M.R., Smellie, J.L., Strelin, J.A., Lawver, L.A. and White W.M. Geochemistry of back arc basin volcanism in Bransfield Strait, Antarctica: Subducted contributions and along-axis variations. *J. Geophys Res.,* **107**: NO. B8, 10.1029/2001JB000444 (2002).
30. Kennish, M.J. and Lutz R.A. Morphology and distribution of lava flows on mid-ocean ridges: a review. *Earth Sci. Rev.,* **43**: 63-90 (1998).
31. Kirkpatrick, R.J. Crystal growth from the melt: a review. Am. Mineralogist **60**: 798-814 (1975).
32. Knipper, A., Ricou, L.E. and Dercourt J. Ophiolites as indicators of the geodynamic evolution of the Tethyan ocean. *Tectonophysics,* **123**: 213-40 (1986).
33. Lipard, S.J., Shelton, A.W. and Gass I.G. The ophiolite of Northern Oman. *Geol. Soc. London Memoir,* **11**: 178

(1986).
34. Lofgren, G.. Experimental studies on the dynamic crystallization of silicate melts, In: Physics of magmatic processes, edited by R.B. Hargraves, (Princeton Univ Press, Princeton), 455-487 (1980).
35. Lofgren, G.E. An experimental study of plagioclase crystal morphology: isothermal crystallization. *Am. J. Sci.,* **274**: 243-273 (1974).
36. Malpas, J., Calon, T.J. and MacDonald R.W.J. The Shulaps ophiolite complex of British Columbia, Canada: a Palaeozoic/Mesozoic arc-related microterrane. In: Ishiwatari, A., et al. (Eds.) Circum-Pacific Ophiolites. Proceedings of the 29th International Geological Congress. Part D. 69-87 (1994).
37. McCall, G.J.H. Explanatory text of the Minab quadrangle map: 1:250000, No. J13, *Geol. Surv. Iran, Tehran,* 530 pp., (1985a).
38. McCall, G.J.H. Explanatory text of the Tahruie quadrangle map: 1:250000, J14, ibid., 454 pp., (1985b).
39. McCall, G.J.H. Explanatory text of the Fannuj quadrangle map: 1:250000, K14, ibid., 409 pp., (1985c).
40. McCall, G.J.H. Area report, East Iran Project, Area No. 1, *Geol. Surv. Iran,* Report No. **57**, 634 pp., (1985e).
41. McCall, G.J.H. The early history of the Earth. *Geoscientist* **6(1)**: 10-14 (1996).
42. McCall, G.J.H. The geotectonic history of the Makran and adjacent areas of southern Iran. *J. Asian Earth Sci.,* **15**: 517-531 (1997).
43. McCall, G.J.H. and kidd R.G.W. The Makran, southeastern Iran: the anatomy of a convergent plate margin active from Cretaceous to present. In: Leggett, J. (Ed), Trenchfore arc geology. *Geol. Soc. London Spec. Publ.,* **10**: 387-97 (1981).
44. Mevel, C. and Velde D. Clinopyroxenes in Mesozoic pillow lavas from the French Alps: influence of cooling rate on compositional trends. *Earth Planet. Sci. Lett.,* **32**: 158-164 (1976).
45. Mislankar, P.G. and Iyer S.D. Petrographical indicators of petrogenesis: Examples from Central Indian Ocean Basin Basalts. *Indian J. Marin. Sci.,* **30**: 1-8 (2001).
46. Miyashiro, A., Shido, F.A. and Ewing M. Crystallization and differentiation in abyssal tholeiites and gabbros from mid-oceanic ridges. *Earth Planet. Sci. Lett.,* **7**: 361-365 (1970).
47. Moore, J.G. Water content of basalt erupted on the ocean floor. *Contrib. Mineral. Petrol.,* **28**: 272-279 (1970).
48. Moore, J.G. Mechanisms of formation of pillow lava. *Am. Sci.,* **63**: 269-277 (1975).
49. Moore, J.G. and Charlton D.W. Ultra thin layers exposed near San Luis Obispo Bay, California. *Geology,* **12**: 542-545 (1984).
50. Mukhopadhyay, R., Batiza, R. and Iyer S.D. Petrology of ancient Central Indian Ocean Basin seamounts: Evidences for near axis origin, *Geo-Mar Lett.,* **15**: 106-110 (1995).
51. Natland, J. Mineralogy and crystallization of oceanic basalts. In Oceanic basalts, edited by F A Floyd, *(Blackie and Son, Glasgow),* 63-93 (1991).
52. Pearc, J.A. Geochemical fingerprinting of oceanic basalts with applications to ophiolite classification and the search for Archean oceanic crust. *Lithos,* **100**: 14-48 (2008).
53. Pearce, J. A., Alabaster, T., Shelton, A.W. and Searle M.P. The Oman ophiolite as a Cretaceous arc-basin complex: evidence and implications. *Philos. Trans. R. Soc. London,* **A300**: 299-317, (1981).
54. Pearce, J.A. Statistical analysis of majore element patterns in basalts. *J. Petrol.,* **17**: 15-43 (1976).
55. Pearce, J.A. Trace element characteristics of lavas from destructive plate boundaries. In: Thrope, R. S. (Ed.), Andesites. John Wiley & Sons, *New York,* 525-548 (1982).
56. Pearce, J.A. and Cann J.R. Tectonic setting of basic volcanic rocks determined using trace element analyses. *Earth Planet. Sci. Lett.,* **12**: 339-49 (1973).
57. Pearce, J.A., Lippart, S. and Roberts S. Characteristic and tectonic setting of Supra-subduction zone ophiolites. *Geol. Soc. Spec. publ. London,* **16**: 77-96 (1984).
58. Pearce, J.A. and Norry M.J. Petrogenetic implications of Ti, Zr, Y and Nb variations in volcanic rocks. *Contrib. Mineral. Petrol.,* **69**: 33-47 (1979).
59. Pearce, J.A. and Peate D.W. Tectonic implications of the composition of volcanic arc magmas. *Ann. Rev. Earth Planet. Sci.,* **23**: 251-285 (1995).
60. Perfit, M.R., Chadwick J. and W.W. Magmatism at mid-ocean ridges; Constraints from volcanological and geochemical investigations. In: Buck, W.R., Delaney, P., Karson, J.A. (Eds.), Faulting and Magmatism at Mid Ocean Ridges. *Geophys Monograph,* American Geophysical Union, Washington, DC, **92**: 59-115 (1998).
61. Rhodes, J.M., Blanchard, D.P., Dungan, M.A., Rodgers, K.V. and Brannon J.C. Chemistry of Leg 45 basalts. In: W.G. Melson, P.D. Rabinowitz et al. (Eds.), Initial Rep. *Deep Sea Drill. Proj.,* **45**: 447-459 (1978).
62. Rhodes, J.M., Dungan, M.A., Blanchard, D.P. and Long P.E. Magma mixing at mid-ocean ridges: Evidence from basalts drilled near 22°N on the mid-Atlantic ridge, *Tectonophys,* **55**: 35-61 (1979).
63. Ricou, L.E. Le croissant ophiolitique peri-arabe: un ceinture de nappes mise en place au Cretace superieur. *Rev. Geogr. Phys. Geol. Dyn.,* **13**: 327-50 (1971).
64. Rittmann, A. Volcanoes and their Activity. John Wiley and Sons, New York (1962).
65. Saunders, A.D. and Tarney J. The geochemistry of basalts from a back-arc spreading centre in the east Scotia sea. *Geochim. Cosmochim. Acta.,* **43**: 555-72 (1979).
66. Saunders, A.D., Tarney, J., Marsh, N.G. and Wood D.A. Ophiolites as an ocean crust or marginal basin crust: A geochemical approach. In: Panayiotou, A. (Ed.), Ophiolites. Proc. Internat. Ophiolite Symp. *Geol. Surv. Dept. Cyprus Nicosia,* 193-204 (1980).
67. Scott, R.B. and Hajash A.J. Initial submarine alteration of basaltic pillow lavas: A microporobe study, *Am. J. Sci.,* **276**: 480-501 (1976).
68. Sengör, A.M.C. The Cimmeride orogenic system and the tectonics of Eurasia. *Geol. Soc. Am. Spec.,* 195 pp., (1984).
69. Sengör, A.M.C. Tectonics of the Tethysides: orogenenic collage development in collisional setting. *Ann. Rev. Earth Planet. Sci.,* **15**: 213-44 (1987).
70. Sengör, A.M.C. A new model for the Late Palaeozoic-Mesozoic tectonic evolution of Iran and implications for Oman. *Geol. Soc. London Spec. Publ.,* **49**: 797-831

(1990).
71. Shervais, J.W. Ti-V plots and the petrogenesis of modern and ophiolitic lavas, *Earth Planet. Sci. Lett.,* **59**: 101-118 (1982).
72. Sinton, J.M., Bergmanis, E., Rubin, K., Batiza, R., Gregg, T.K.P., Grönvold, K., Macdonald, K. and White S. Volcanic eruptions on mid-ocean ridges: new evidence from the superfast-spreading East Pacific Rise, 17°-19° S. *J. Geophys. Res.,* 107 (B6) (2002).
73. Smewing, J.D. and Potts P.J. Rare earth abundances in basalts and metabasalts from the Troodos Massif, Cyprus, *Contrib. Mineral. Petrol.,* **57**: 245-58 (1976).
74. Snavely, P.D., MacLeod, N.S. and Wagner H.C. Miocene tholeiitic basalts of coastal Oregon and Washington and their relations to coeval basalts of the Columbia Plateau. *Geol. Soc. Am. Bull.,* **84**: 387-424 (1973).
75. Solomon, M. The nature and possible origin of the pillow lavas and hyaloclastite breccias of King Island, Australia. *Geol. Soc. London Quarterly Journal*. **124**: 159-169 (1969).
76. Spooner, E.T.C. and Fyfe W.S. Sub-sea-floor metamorphism, heat and mass transfer. *Contrib. Mineral. Petrol.,* **42**: 287-304 (1973).
77. Sun, S.S. and McDonough W.F. Chemical and isotopic systematics of oceanic basalts: implications for mantle compositions and processes. In: Saunders, A.D., Norry, M.J. (Eds.), Magmatism in the Ocean Basins. *Geol. Soc. Spec. Publ.,* **42**: 313-345 (1989).
78. Sun, S.S. and Nesbitt R.W. Geochemical characteristics of mid oceanic ridge basalts. *Earth Planet. Sci. Lett.,* **44**: 119-138 (1979).
79. Swanson, D.A. Pahoehoe flows from the 1969-1971 Mauna Ulu eruption, Kilauea Volcano, Hawaii. *Bull Geol Soc Am.,* **84**: 615-626 (1973).
80. Swanson, S.E. and Schiffman P. Textural evolution and metamorphism of pillow basalts from the Franciscan Complex, Western Matin County, California. *Contrib. Mineral. Petrol.,* **69**: 291-299 (1979).
81. Tirrul, R., Bell, I.R., Griffs, R.J. and Camp V.E. The Sistan suture zone of eastern Iran. *Bull. Geol. Soc. Am.,* **94**: 134-50 (1983).
82. Venturellie, G., Thrope, R.S. and Potts P.j. Rare earth and trace element characteristics of ophiolitic metabasalts from the Alpine-Apennine. *Earth Planet. Sci. Lett.,* **53**: 109-23 (1981).
83. Walker, G.P.L. Morphometric study of pillow size spectrum among pillow lavas. *Bull. Volcanol.,* **54**: 459-474 (1992).
84. Wang, Z., Wilde, S.A., Wang, K. and Yu L. A MORB-arc basalt-adakite association in the 2.5 Ga Wutai greenstone belt: late Archean magmatism and crustal growth in the North China Craton, *Precambrian. Res.,* **131**: 323-343 (2004).
85. Winchester, J.A. and Floyd P.A. Geochemical discrimination of different magma series and their differentiation products using immobile elements. *Chem. Geol.,* **20**: 325-343 (1979).
86. Wood, D.A., Joron, J.L. and Treuil M. A re-appraisal of the use of trace elements to classify and discriminate between magma series erupted in different tectonic settings. *Earth Planet. Sci. Lett.,* **45**: 326-336 (1979).
87. Yamagishi, H. Growth of pillow lobes-evidence from pillow lavas of Hokkaido, Japan and North Island New Zealand. *Geology,* **13**: 499-502 (1985).
88. Yuan, C., Sun, M., Zhou, M.F., Xiao, W. and Zhou H. Geochemistry and petrogenesis of the Yishak Volcanic Sequence, Kudi ophiolite, West Kunlun (NW China): implications. For the magmatic evolution in a subduction zone environment. *Contrib. Mineral. Petrol.,* **150**: 195–211 (2005).